Intermetallics 88 (2017) 41–45

Contents lists available at ScienceDirect

Intermetallics

journal homepage: www.elsevier.com/locate/intermet

Synthesis and magnetocaloric characterization of rapidly solidified $ErMn_2$ melt-spun ribbons

J.L. Sánchez Llamazares[a,*], P. Ibarra-Gaytán[a], C.F. Sánchez-Valdés[b], P. Álvarez-Alonso[c], A.D. Martínez-Iniesta[d]

[a] Instituto Potosino de Investigación Científica y Tecnológica A.C., Camino a la Presa San José 2055, Col. Lomas 4ª, 78216 San Luis Potosí, S.L.P., Mexico
[b] División Multidisciplinaria, Ciudad Universitaria, Universidad Autónoma de Ciudad Juárez (UACJ), calle José de Jesús Macías Delgado # 18100, 32579 Ciudad Juárez, Chihuahua, Mexico
[c] Departamento de Física, Universidad de Oviedo, 33007 Oviedo, Spain
[d] Universidad Tecnológica de Tula-Tepeji, Av. Universidad Tecnológica No. 1000, C.P. 42830, El Carmen, Tula de Allende, Hidalgo, Mexico

ARTICLE INFO

Keywords:
$ErMn_2$ Laves phase
Melt spun ribbons
Magnetocaloric effect
Magnetic entropy change
Adiabatic temperature change

ABSTRACT

We have fabricated melt-spun ribbons of nominal composition $ErMn_2$ and studied their phase constitution and magnetocaloric (MC) properties by X-ray diffraction, scanning electron microscopy (SEM), magnetization and heat capacity measurements. The major phase formed shows the $MgZn_2$-type hexagonal structure (C14-type); however, both XRD and SEM analyses revealed the formation of impurity phases (*i.e.*, Er_6Mn_{23} and $ErMn_{12}$). Ribbons exhibit a saturation magnetization of 149 Am^2kg^{-1} at 2 K and a Curie temperature of T_C = 15 K. A field-induced metamagnetic transition at very low critical magnetic fields was observed below 8 K that leads to a change of sign in the magnetic entropy change ΔS_M below this temperature ($\Delta S_M{}^{peak}$ = 2.5 $Jkg^{-1}K^{-1}$ at 2 K and 5 T). For a magnetic field change of 5 T (2 T) applied along the ribbon length, the samples show a large peak value of the magnetic entropy change $\Delta S_M{}^{peak}$ of −20.5 (−10.8) $Jkg^{-1}K^{-1}$, a full-width at half-maximum δT_{FWHM} for the $\Delta S_M(T)$ curve of 20 (12) K, and a maximum adiabatic temperature change $\Delta T_{ad}{}^{max}$ of 7.4 (3.6) K. The obtained results are compared with the reported in literature by other authors for bulk alloys.

1. Introduction

Magnetic refrigeration, an alternative cooling technology with a range of applications from room temperature to helium and hydrogen liquefaction temperatures [1], has boosted the interest in the magnetocaloric effect, characterized by the temperature and magnetic entropy changes occurring in the magnetic material when applying (or removing) an external magnetic field under adiabatic or isothermal conditions, respectively. Together with these properties, a key parameter for comparing MC materials is the refrigerant capacity (*RC*), which estimates the interchangeable heat between the refrigerant material and the reservoirs if an ideal refrigerant cycle is considered. This physical quantity is significant when the material shows sizeable maximum values of both the adiabatic temperature and magnetic entropy changes.

The MC properties of binary Laves phases based on rare-earths (R) have been extensively investigated due to their potential as magnetic refrigerants in the cryogenic temperature range [1–5]. Up to now, most studies have been focused mainly on RM_2 compounds with M = Al, Ni, and Co. However, recent work authored by Zuo et al. have reported a large reversible magnetic entropy change ΔS_M in RMn_2 compounds with several heavy R metals, such as Tb, Dy, Ho, and Er, underlying that they can be also considered promising working MC substances in the 10–80 K range [5]. It is important to note that the maximum adiabatic temperature change $\Delta T_{ad}{}^{max}$ for RMn_2 compounds has not been estimated yet. For bulk $ErMn_2$ alloys produced after a prolonged thermal annealing (1073 K; 7 days), they measured large values of the maximum magnetic entropy change $\Delta S_M{}^{peak}$ and *RC* (*i.e.*, −25.5 (−13.4) $Jkg^{-1}K^{-1}$ and 316 (100) Jkg^{-1}, respectively, for a magnetic field change $\mu_o\Delta H$ of 5 T (2 T); *RC* was estimated integrating the area below the full-width at half-maximum of the $\Delta S_M(T)$ curve). Present contribution focuses on this intermetallic alloy that crystallizes in the hexagonal $MgZn_2$-type structure of the Laves phases (C-14; space group P63/mmc, number 194) [6,7]. In this compound, only Er atoms carry magnetic moment (*i.e.*, that of Mn is almost zero), which is close to that of free Er^{3+} ion (~8.8 versus 9 μ_B/f.u., respectively) [8,9]; Er^{3+} moments couple ferromagnetically through RKKY interaction below a Curie temperature T_C of 15 K [10]. Magnetization studies conducted on

* Corresponding author.
E-mail address: jose.sanchez@ipicyt.edu.mx (J.L. Sánchez Llamazares).

http://dx.doi.org/10.1016/j.intermet.2017.05.001
Received 22 January 2017; Received in revised form 17 April 2017; Accepted 3 May 2017

single crystals grown by Bridgman method show that the *c*-axis is the easy magnetization direction [9], and the saturation magnetization is reduced along the a and b axes; furthermore, if a magnetic field is applied along *a* and *b* axes, a critical magnetic field of ~1.2 T induces a metamagnetic transition that reorients the magnetic moments in a canted magnetic structure in which they tilt alternatively ± 30° from the a (*b*) axis in the *a*-*c* (*b*-*c*) plane [9]. In a more recent study, carried out on single crystal grown by Czochralski method [10], is reported that the critical field that induces the transition along the *a*-axis is reduced to 0.7 T.

Rapid solidification by melt spinning technique has been effectively applied in the last few years to produce different crystalline R-based MC materials, such as $LaFe_{13-x}Si_x$ [11], $Gd_5(SiGeSn)_4$ [12], RNi_2 (R = Tb, Dy) [13–15], $NdPrFe_{17}$ [16], Dy_3Co [17], and DyNi [18]. In most of the cases, a single phase is formed in the as-solidified alloy ribbons, or after a much shortened annealing compared to their bulk counterparts. The aim of the present investigation has been to study the MC behavior of $ErMn_2$ melt-spun ribbons. Their MC properties were determined from both magnetization and heat capacity measurements; the results are compared with those obtained for bulk samples.

2. Experimental procedures

Ribbon flake samples were fabricated from a bulk Ar arc melted pellet of nominal composition $ErMn_2$; highly pure Er (99.9 %, Sigma-Aldrich) and Mn (99.998 %, Alfa Aesar) were used as raw materials. Samples were melted three times to ensure an adequate starting homogeneity; special care was taken to keep the 1:2 composition in the starting master alloys. Rapid solidification process was carried under UHP Ar atmosphere using an Edmund Bühler SC melt spinner system; once molten, the alloy was ejected onto the polished surface of a copper wheel rotating at a surface linear speed of 15 ms^{-1}.

X-ray diffraction (XRD) patterns of finely powdered samples were collected with a Rigaku smartlab high-resolution diffractometer using Cu-K_α radiation (λ = 1.5418 Å); the ribbons were grounded using an agate mortar. The scan was carried out in the interval $15° \leq 2\theta \leq 100°$ with 0.01° of step increment. Microstructure was studied with a dual beam Helios Nanolab, ESEM FEI Quanta 200 equipped with an energy dispersive spectroscopy (EDS) system.

Magnetic measurements were performed by vibrating sample magnetometry in a Quantum Design PPMS® Dynacool®-9T system; the typical size of the measured sample was 3.5 mm in length and 0.6 mm in width. The magnetic field $\mu_o H$ was applied along the ribbon axis (*i.e.*, the direction of ribbon formation or longitudinal direction) to minimize the effect of the internal demagnetizing field. The low-field (5 mT) magnetization as a function of temperature curve $M(T)$ was measured between 2 and 100 K under zero-field-cooled (ZFC) and field-cooled (FC) regimens, respectively, where $M_{FC}(T)$ curve was used to estimate the T_C value while the high-field $M(T)$ curve was measured on heating (FH) under $\mu_o H$ = 5 T; all $M(T)$ curves were measured with a temperature sweeping rate of 1.0 $Kmin^{-1}$. Heat capacity (HC) as a function of temperature was measured by means of the relaxation method using the HC option of a Quantum Design PPMS® Evercool®-9T system. Measurements were performed using the vertical HC puck. Thus, as for magnetization measurements, the magnetic field was applied along the ribbon major length. $\Delta S_M(T)$ curves were obtained from: (i) numerical integration of the Maxwell relation, *i.e.*, $\Delta S_M(T, \mu_o H) = \mu_o \int_0^{\mu_o H_{max}} [\frac{\partial M(T, \mu_o H')}{\partial T}]_{\mu_o H'} dH'$; (ii) total entropy change $S_T(T)$ curves obtained from the specific heat $c_p(T,\mu_o H)$ curves measured at 0, 2 and 5 T. The adiabatic temperature change as a function of temperature and applied magnetic field change $\Delta T_{ad}(T,\mu_o \Delta H)$ curves were indirectly obtained from the total $S_T(T,\mu_o H)$ curves.

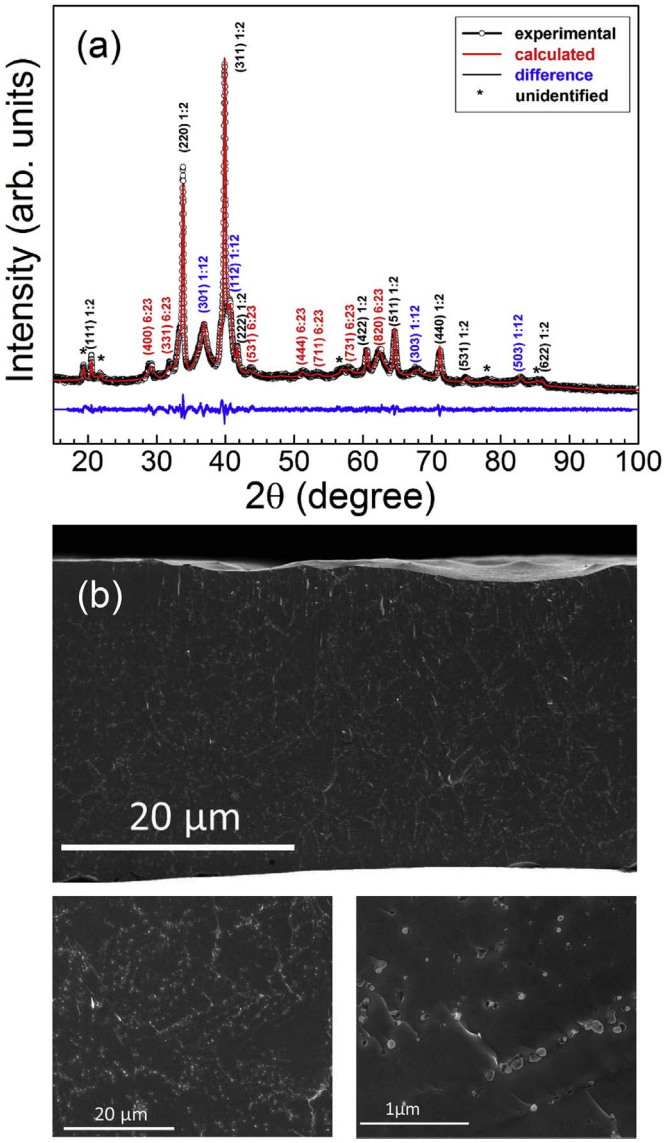

Fig. 1. (a) Le Bail profile fitting of the XRD pattern of as-solidified $ErMn_2$ ribbons (CuK_α). The major phase shows the $MgZn_2$-type hexagonal structure of the Laves phases (C14; $a = b$ = 0.52989(1) nm; c = 0.86516(2) nm); the diffraction lines of 6:23 and 1:12 phases are also present. (b) SEM micrographs of the cross-section and typical microstructure shown by as-solidified $ErMn_2$ melt-spun ribbons.

3. Results and discussion

The indexed room temperature XRD pattern of the as-quenched ribbons is depicted in Fig. 1(a). Its Le Bail profile fitting was done using the FullProf Suite package [19]. The Bragg reflections of the major phase performed correspond to a hexagonal $MgZn_2$-type crystal structure of the Laves phases (C-14; space group $P6_3/mmc$, number 194), with lattice parameters $a = b$ = 0.52989(1) nm and c = 0.86516(2) nm, which are in good agreement with the reported for bulk alloys [5,10,20]. The additional minor intensity XRD peaks of the experimental pattern belong to 6:23 and 1:12 phases. Both are stable phases of the binary Er-Mn phase diagram [21]. It must be noticed that the peaks appearing in the pattern show a noticeable broadening; this suggest that the rapid solidification process alters the local structural equilibrium order. Fig. 1(b) shows typical SEM micrographs at different magnifications of the ribbon's fracture microstructure. While their thickness is around 30 µm, the major phase crystallizes into micronic in size grains with no preferred orientation with respect to both ribbon surfaces. It is worth noting that, in agreement with XRD analysis, the